Modification of Condensation Heat Transfer Model for the MARS Code in the Presence of Noncondensable Gases

Jun Yeob Lee [a*], Jee Min Yoo [a], Byong Jo Yun [a], Jae Jun Jeong [a]
[a]*Mechanical Engineering Dept., Pusan Nat'l Univ., Jangjeon-2-Dong, Geumjeong-Gu, Busan, Korea*
[*]*Corresponding author: 0629jy@pusan.ac.kr*

1. Introduction

Condensation is a very effective way of heat removal and therefore is widely used in various thermal-hydraulic systems including a nuclear power plant. For example, some passive safety systems (e.g. passive containment cooling system, PCCS), which are adopted in an advanced reactor, take advantage of it. Also, the condensation on the containment wall during a loss-of-coolant accident can help to maintain the integrity of the containment with its excellent heat removal capability.

Most of condensation in nuclear power plants occur in the presence of noncondensable gases. Even very small amounts of noncondensable gases contained, condensation rate is greatly reduced. Therefore, without accurate prediction for the effect of noncondensable gases, a proper safety analysis and design of safety system using condensation cannot be obtained.

A thermal hydraulic systems analysis code, MARS, includes a condensation heat transfer model which can consider the effect of noncondensable gases. However, the model has some limitations in predicting condensation in the presence of noncondensable gases.

In this study, a new model for condensation in the presence of noncondensable gases has been developed and implemented into the MARS code. The new model has been evaluated using several experimental data sets for condensation mainly focused on the thermal hydraulic conditions in a nuclear reactor containment building during a loss-of-coolant accident(LOCA).

2. Development of a new model for condensation in the presence of noncondensable gases

2.1 Diffusion layer model

Fig. 1 shows that condensation phenomenon in the presence of noncondensable gases schematically. As condensation proceeds, the noncondensable gases accumulates near the vapor/liquid interface and forms a layer, called diffusion layer. This layer acts as a thermal resistance because the accumulated noncondensable gases decreases saturation temperature near the interface.

Peterson et al.[1] developed a theoretical model for condensation in the presence of noncondensable gases using diffusion layer theory and introducing the concept of condensation thermal conductivity. It is derived from the molar-based Fick's law with the Clausius-Clapeyron equation and the ideal gas law. One of the advantage of this model is that latent heat transfer and sensible heat

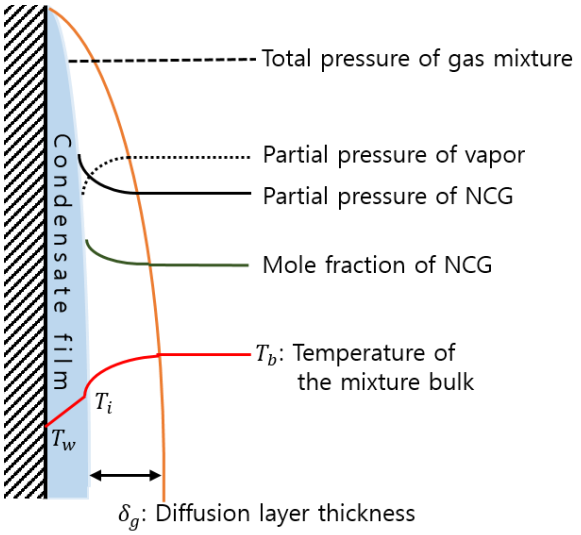

Fig. 1. Schematic illustration of diffusion layer

transfer can be expressed as combined form in series with the film heat transfer.

$$q_t'' = h_f\left(T_i - T_w\right) = \left(h_c + h_s\right)\left(T_b - T_i\right) \qquad (1)$$

Sensible heat transfer coefficient is expressed in the form of the Nusselt number and latent heat transfer coefficient is expressed in the form of the Sherwood number:

$$Nu = \frac{h_s \cdot L}{k_g},\ Sh = \frac{h_c \cdot L}{k_c}, \qquad (2)$$

where k_c is the condensation thermal conductivity and defined as:

$$k_{c,Peterson} = \frac{1}{\phi}\frac{h'_{fg}\, h_{fg} PDM_v^{\,2}}{R^2 \overline{T}^3}. \qquad (3)$$

Herranz et al. [2] has extended Peterson's diffusion layer model to deal with variation of thermal properties in diffusion layer due to large gas-wall temperature differences. The condensation thermal conductivity of Herranz's diffusion layer model is:

$$k_{c,\mathrm{Herranz}} = \frac{1}{\phi \overline{T}}\frac{h'_{fg}\, h_{fg} PDM_v^{\,2}}{R^2 T_i T_b}. \qquad (4)$$

2.2 Condensation model with turbulent diffusion coefficient

The diffusion layer models are generally derived based on the stagnant film model. In the models, mass transport is divided into the diffusive transport due to

molecular diffusion in the direction of perpendicular to condensing surface and advective transport due to flow itself. A longitudinal diffusion, which is proportional to mass concentration distribution to axial direction, and a parallel flow to the condensate are ignored. However, in practice, these transport phenomena affect mass transfer rate in condensation considerably because of shear stress induced by friction between the mixture gas and the condensate.

The additional mass transfer term can be obtained by solving the equation for conservation of species using mass concentration and velocity variables decomposed into the mean part and the fluctuating part($u = \bar{u} + u'$) [3].

$$\frac{\partial \bar{c}}{\partial t} + \bar{u}_j \frac{\partial \bar{c}}{\partial x_j} = \frac{\partial}{\partial x_j}\left(D\frac{\partial \bar{c}}{\partial x_j} - \overline{u_j' c'} \right). \quad (5)$$

The terms in the parentheses of the right-hand side of Eq. (5) represent the molar flux of noncondensable gases to the direction of the condensate. It can be rewritten as:

$$j_v^* = D\frac{\partial \bar{c}}{\partial y} - \overline{u'c'}. \quad (6)$$

The Reynolds stress term in the right-hand side of Eq. (6) represents the additional mass transfer by turbulent flow and it can be calculated using the Prandtl's turbulent mixing model.

$$-\overline{u'c'} = l_m^2 \left|\frac{\partial \bar{u}}{\partial y}\right| \frac{\partial \bar{c}}{\partial y}. \quad (7)$$

the product of mean velocity gradient and the mixing length can be expressed as the turbulent diffusion coefficient, D_{turb}:

$$D_{turb} = l_m^2 \left|\frac{\partial \bar{u}}{\partial y}\right|. \quad (8)$$

The mixing length l_m is determined using Cebeci's Van-Driest type mixing length model, presented in Table I. The boundary between the inner region and the outer region is the y-point at which the turbulent diffusion coefficients determined for each region are equal [4].

The velocity gradient in the right-hand side of Eq. (8) is obtained by differentiating the velocity profile defined by the law of the wall. The viscous sublayer is up to y^+=10.8. In the region of y^+>10.8, velocity profile of the logarithmic region is used. The buffer layer is not considered in the present model.

For the convenience of utilization, the turbulent diffusion coefficient is averaged over the diffusion layer, called the depth-averaged turbulent diffusion coefficient, $\overline{D_{turb}}$.

$$\overline{D_{turb}} = \frac{1}{\delta_g}\int_0^{\delta_g} l_m^2 \left|\frac{\partial \bar{u}}{\partial y}\right| dy. \quad (9)$$

Summation of the molecular diffusion coefficient and the depth-averaged turbulent diffusion coefficient is called the effective diffusion coefficient and expressed as:

$$D_{eff} = D + \overline{D_{turb}}. \quad (10)$$

Table I: Turbulent mixing length model of Cebeci et al.

Inner region	Outer region
$l_m = \kappa y\left[1-\exp\left(-y^+/A^+\right)\right]$	$D_{turb} = \frac{0.0168 U_\infty \delta_1}{\left[1+5.5\left(y/\delta\right)^6\right]}$
$\kappa = 0.41$ $A^+ = 26/\exp\left(5.9m^+\right)$ $y^+ = yu^*/\nu$. $m^+ = \nu_l/u^*$. $u^* = \sqrt{\tau_i/\rho}$	δ_1 : the displacement thickness δ : the boundary layer thickness U_∞ : velocity of bulk mixture

The present condensation model is based on the diffusion layer model of Peterson et al. The condensation thermal conductivity derived by Herranz is used and, in addition, its molecular diffusion coefficient is replaced with the effective diffusion coefficient obtained in this study.

$$k_{c,\text{present}} = \frac{1}{\phi\bar{T}} \frac{h'_{fg} h_{fg} P\left(D + \overline{D_{turb}}\right) M_v^{\,2}}{R^2 T_i T_b}. \quad (11)$$

Using the heat and mass transfer analogy, correlations for the Nusselt number and the Sherwood number are presented in Table II. The correlations are suited for the convection heat transfer on vertical surface and the local heat transfer coefficient.

The Nusselt number for sensible heat transfer is corrected by a suction factor and a fog formation factor given by Brouwers[5]. To consider the superheated vapor effect, a correction factor derived empirically using COPAIN data is applied.

$$Nu = Nu_0 \times f\left(\Delta T_{\text{sup}}\right), \quad Sh = Sh_0 \times f\left(\Delta T_{\text{sup}}\right). \quad (12)$$

$$f\left(\Delta T_{\text{sup}}\right) = \frac{1}{1+0.0032\Delta T_{\text{sup}}^{\,2.4214}}. \quad (13)$$

3. Evaluation of the MARS code with the present model

The condensation heat transfer model of the MARS code and the new model has been evaluated against local heat transfer coefficient data and heat flux data for experiments of condensation on vertical surface in the present of noncondensable gases.

3.1 Experiments for condensation on vertical surface

The present model is developed to predict condensation heat transfer in the containment after a LOCA, where forced convection flow is dominant

inside the containment. Shortly after that, natural convection flow is getting dominant. Experimental data to be selected should be able to cover the flow conditions of the condensation in the containment after a LOCA.

Table II: Correlations for the Nusselt number and the Sherwood number

.	Flow condition	Flow regime	Correlation for local value
Nu	External forced convection	Turbulent	$0.0296Re^{4/5}Pr^{1/3}$
		Laminar	$0.332Re^{1/2}Pr^{1/3}$
	External natural convection	Turbulent	$0.082(GrPr)^{1/3} \times\left(-9+2.4\frac{T_w}{T_\infty}-0.5\frac{T_w}{T_\infty}^2\right)$
		Laminar	$0.4425(GrPr)^{1/4}$
Sh	External forced convection	Turbulent	$0.0296Re^{4/5}Sc^{1/3}$
		Laminar	$0.332Re^{1/2}Sc^{1/3}$
	External natural convection	Turbulent	$0.082(GrSc)^{1/3} \times\left(-9+2.4\frac{T_w}{T_\infty}-0.5\frac{T_w}{T_\infty}^2\right)$
		Laminar	$0.4425(GrSc)^{1/4}$

The data set of CONAN [5], COPAIN [6], Park's experiments [7] were selected for the evaluation of the MARS code with the present model because these experiments cover those flow conditions. In the entrance region of the test section, the flow condition is mostly forced convection flow. Along the distance from the inlet, it turns to mixed convection flow or natural convection flow as buoyancy effect getting dominant. Also, the experimental data sets cover thermal-hydraulic conditions in the containment such as pressure, mole fraction of noncondensable gases, temperature, and so on. Specific test matrix of the database is presented in Table III.

The CONAN experiment facility includes a square cross section channel. One of the channel surface is condensation wall cooled by flowing coolant. The test section of COPAIN experiment and of Park's experiment have similar geometry to the test section of CONAN experiment and only have different size of its test sections. Thus, in the analyses, only the number of the volumes assigned to simulate the test section is changed for each experiment.

3.2 Evaluation results

Fig. 2 shows a comparison of the measured and calculated heat flux for COPAIN and CONAN data set. Fig. 3 shows a comparison of the measured and calculated heat transfer coefficient for Park's experimental data set. The standard deviation is used to evaluate the present model quantitatively, and defined as:

$$STD=\sqrt{\sum\left(\frac{M_i-C_i}{M_i}\right)^2/(N-1)} \quad , \qquad (14)$$

where M_i represents a measured value, C_i represents a calculated value, and N represents the number of data point.

The present model has better prediction ability compare to the original model of MARS for both local heat flux and local heat transfer coefficient. The STDs obtained from the evaluation results for each experimental data set are presented in Fig.2 and Fig.3.

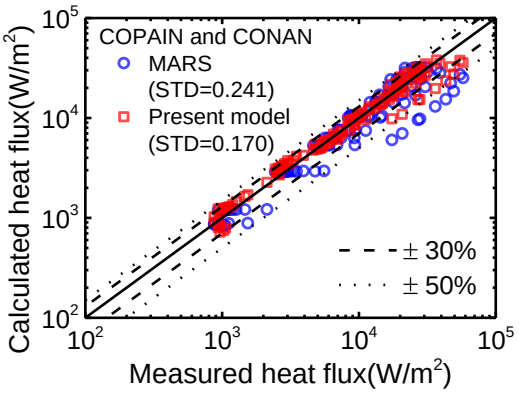

Fig. 2. Comparison of measured and calculated local heat flux for COPAIN and CONAN experiment data

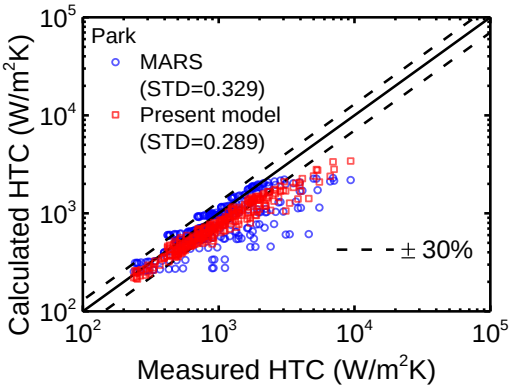

Fig. 3. Comparison of measured and calculated local heat transfer coefficient for Park's experiment data

The remarkable improvement of the present model compared to the original model of MARS is the ability to predict a local condensation heat transfer rate. In the entrance region of the condensation surface, heat transfer rate and condensation rate is very high and tend to decrease along the distance from the inlet. The original model of the MARS is not able to predict the tendency. The first reason of the defect is that the correlations for the Nusselt number and the Sherwood number used in the model are derived for the average heat transfer coefficient and mass transfer coefficient. The second reason is that the characteristic length used

Table III: Test Matrix for the Evaluation

Exp.	Shape and Orientation	Mass fraction of NCG	Pressure [bar]	Inlet velo- city [m/s]	Wall subcooling [K]	Thermal state
CONAN	Vertical plate	0.114~0.886	1.0	2.48~2.63	18~35	Saturated
COPAIN	Vertical plate	0.767~0.867	1.02~1.21	0.3~0.52	22~52	Superheated
Park	Vertical plate	0.2~0.7	1.0	1.4~7.0	17~50	Saturated

in the original model is inappropriate for a calculation of convection heat transfer. On the other hand, in the present model, the correlations for the Nusselt number and the Sherwood number derived for the local heat transfer coefficient and mass transfer coefficient are adopted, and the distance from the inlet is used as a characteristic length. And the additional mass transfer term corrects condensation heat transfer for the entire region. As a result, Fig. 4 shows that the present model can predict well the heat transfer tendency in the entrance region.

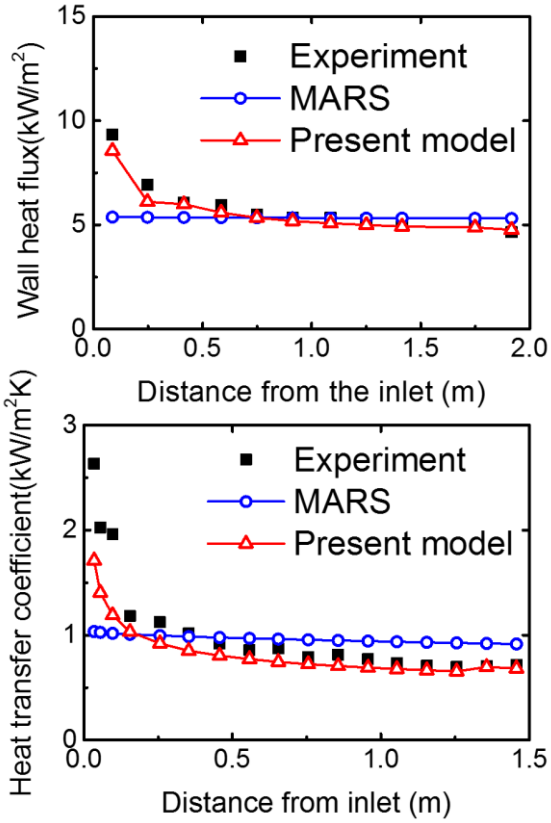

Fig. 4. Comparison of the original model and the present model with the experimental data sets; COPAIN(top), and Park's experiment(bottom)

4. Conclusions

A new condensation heat transfer model based on the diffusion model of Peterson has been developed and implemented into the MARS code.

In the present condensation heat transfer model, the additional mass transfer induced by longitudinal flow has been considered using the theory of turbulent diffusion with the effective diffusion coefficient. The result of the evaluation shows that the present model shows better prediction than the original model of MARS code for the entrance region as well as the overall region. It implies that the additional mass transfer term corrects heat and mass transfer well for condensation in the presence of noncondensable gases. Also, it has a different value for local point so that can compensate local value of mass transfer well.

Meanwhile, for some experiment cases with inlet mixture velocity greater than 5m/s, the heat transfer coefficients calculated using the present model are lower than the measured heat transfer coefficients about 20%. However, although the present model predicts well the trend of heat transfer in the entrance region, its predicted values are still much lower than the measured values at. In further study, these deficiencies are should be complemented.

Acknowledgement

This work was supported by the Nuclear Safety Research Program through the Korea Foundation Of Nuclear Safety (KoFONS), granted financial resource from the Nuclear Safety and Security Commission (NSSC), Republic of Korea (No. 1305011).

REFERENCES

[1] P.F. Peterson et al., Diffusion layer theory for turbulent vapor condensation with noncondensable gases, Journal of Heat Transfer, Vol. 115, pp. 998-1003, 1993
[2] L.H. Herranz et al., A diffusion layer model for steam condensation within the AP600 containment, Nuclear Engineering and Design, Vol. 183, pp. 133-150, 1998.
[3] P.J.W. Roberts et al., Turbulent diffusion, Environmental Fluid Mechanics: Theories and Applications, Ch. 2, pp. 7-45, 2002.
[4] W.P. Jones et al., Condensation from a turbulent stream onto a vertical surface, International Journal of Heat and Mass Transfer, Vol. 17, pp. 1019-1028, 1974.
[5] H.J. Brouwers, Effect of Fog Formation on Turbulent Vapor Condensation with Noncondensable Gases, ASME Journal of Heat transfer, Vol. 118, pp. 243-245, 1996.
[6] L. Vyskocil et al., CFD simulation of air-steam flow with condensation, Nuclear Engineering and Design, Vol. 279, pp. 147-157, 2014.
[7] S. Mimouni et al., CFD modelling of wall steam condensation by a two-phase flow approach, Nuclear Engineering and Design, Vol. 241, pp. 4445-4455, 2011.
[8] S.K. Park, Effects of wavy interface on film condensation of steam/air mixture on a vertical surface, Pohang University of Science & Technology, Ph.D Thesis, 1996.